Deeply bound pionic atoms via the (π^-, p) reaction

W. B. Kaufmann
Arizona State University, Tempe, Arizona 85287

P. B. Siegel
California State Polytechnic University Pomona, Pomona, California 91768

W. R. Gibbs
Los Alamos National Laboratory, Los Alamos, New Mexico 87545
and New Mexico State University, Las Cruces, New Mexico 88003

(Received 6 March 1992)

We examine the essentials of the pion capture reaction (π^-, p) with the pion captured directly into an atomic orbit. The reaction is a promising candidate for the population of the $1s$ or $2p$ atomic levels of medium to heavy nuclei. These levels have never been observed, but rather reliable theoretical calculations indicate that they have relatively small widths. One reason for interest in these levels is that they give a direct measurement of the threshold pion-nucleus amplitude, which has a bearing on questions such as chiral-symmetry breaking in the nuclear medium and the anomalously small level shifts and widths of some of the more deeply-bound pionic atoms. The differential cross section for the process is calculated using the distorted-wave impulse approximation. It is found that for medium-mass nuclei and incident pion beams of 20–50 MeV cross sections of the order of microbarns, well within the capability of present meson factories, can be expected. The related process (π^-, n) is also studied.

PACS number(s): 36.10.Gv, 25.80.Hp

I. INTRODUCTION

One of the few methods of studying the threshold pion-nucleus interaction is through the investigation of the atomic energy levels of pionic atoms. This subject has a long history dating from the experimental discovery in 1952 [1]. We begin with a brief review of the customary production of these atoms.

A negative pion that is stopped in a target is normally captured into a highly excited atomic orbit through the Auger emission of an orbital electron. This pionic atom deexcites ("cascades") through electromagnetic transitions, largely x-ray dipole radiation and further Auger emission. The energies of the atomic levels are inferred from the measured x-ray spectrum. Under the influence of the strong interactions, the levels are shifted from the values calculated with only the Coulomb interaction. Furthermore, they acquire a width (in addition to the radiative width corresponding to the x-ray cascade transitions) that reflects the annihilation of the pion on the nucleus. These level shifts and widths bear the imprint of the strong interactions and are important in characterizing the threshold pion-nucleus optical potential.

The atomic level width is roughly proportional to the overlap of the nuclear and atomic wave functions. As can be inferred from the atomic and nuclear sizes plotted in Fig. 1 the width of the occupied level increases rapidly as the cascade develops and n decreases. The cascade ends abruptly when the pion reaches a level for which the strong-interaction width is significantly larger than the radiative width. Because atoms with larger Z have smaller radii, the demise of the cascade occurs at a higher value of n for these atoms. For pionic atoms with light nuclei, the pion often reaches the $1s$ level, from which it annihilates on the nucleus. For nuclei with Z greater

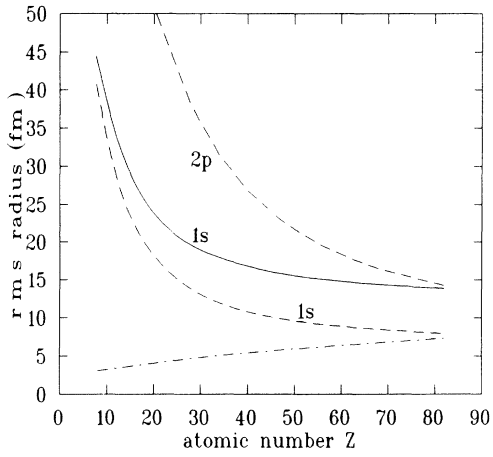

FIG. 1. Radii of pionic atoms in the $1s$ and $2p$ level. The dashed curves contain only the Coulomb interaction, but take into account the finite size of the nucleus. The solid line includes both Coulomb and strong interactions. The dash-dot line is a typical nuclear radius ($1.2A^{1/3}$ fm). Even for the $1s$ levels of very large nuclei, the rms radii of pionic atoms are much larger than the nucleus, provided that the (repulsive) strong interactions are included. For each Z a value of A was chosen to correspond to a "typical" stable nucleus.

than roughly 12 the strong-interaction width of the $2p$ [2] level is sufficiently greater than the x-ray radiative width that the pion is nearly always absorbed by strong processes before it reaches the 1s level. If Z is greater than about forty the cascade usually ends before the $2p$ level is reached. For still larger nuclear species even the $3d$ level is seldom populated. While these limits have been vigorously pushed in recent experiments [3], it is extremely unlikely that experiments depending on the cascade process will ever detect the $1s$ level in a medium mass nucleus such as Ni.

Despite the fact that the $1s$ state of a medium mass nucleus is not populated by the cascade process, the state may be physically real, in the sense that the line width is small compared with the atomic level spacing. Toki, Yamazaki, and their co-workers [4–6] have emphasized that the atomic level widths in the $1s$ states are predicted to be narrow because the repulsive s-wave pion-nucleus optical potential tends to expel the pionic wave function from the nucleus, lowering the probability for pion annihilation.

As the $1s$ level is not populated by the cascade process in all but the lightest nuclei, and because it would be an ideal probe of the low-energy pion-nuclear interaction, it is desirable to form the atoms by some alternative mechanism. Numerous reactions [4–13] for producing pions directly into the deeply bound levels have been proposed over the years. While some may be promising, none has yet led to an experiment which has detected deeply bound pion atomic states.

In this article we will concentrate on the recently proposed direct-capture process

$$\pi^- + (N, Z+1) \rightarrow p + (N, Z)_{\pi^-}, \tag{1}$$

where the subscript π^- refers to the pion in an atomic state [14]. The incident pion strikes a proton, knocking it out of the nucleus; in the process the pion is directly captured into the $1s$ (or $2p$) atomic orbital. The mechanism has the advantage that the pion is already present in the initial state, and the cross section may be calculated fairly reliably through the distorted-wave impulse approximation (DWIA).

The signature of this process is a peak in the knockout proton spectrum. A key question, which can be answered only by further experiments, is whether the knockout proton can be distinguished from the protons ejected in the cascade following the absorption of a pion on nuclei. Experiments to study this background are being planned [15].

The analysis is simplified by the two-body nature of the process. This reaction is analogous to the $(\overline{p},p)$ reaction we suggested earlier for the population of low-lying $\overline{p}$ atomic levels [16], but unlike that process, the (π^-,p) reaction has nonzero momentum transfer even for forward proton knockout. Fortunately, the momentum transfer is small enough that it may be compensated by the Fermi momentum of the struck proton, so that the cross section is not strongly suppressed. In fact, the moderate momentum transfer can be an advantage since it favors the knockout of a nucleon from higher angular-momentum states, which can have higher occupancies.

An additional advantage of pion-capture reactions over a cascade process is that the atomic state can also be formed with the nucleus in an excited state, providing a measure of the optical potential of a pion interacting with an excited nucleus. (As is well known, such atoms might occasionally be formed in a cascade if an atomic transition energy is equal to an excitation energy of the nucleus.)

The only published experimental search for deeply bound pionic states of which we are aware is that of Iwasaki *et al.* [17], which uses the reaction $(n,p\pi)$ with the pion produced directly in an atomic orbit. The experiment, performed at TRIUMF, utilized a monoenergetic beam of 418 MeV neutrons. The predicted cross section (by a DWIA calcuation) is of the order of 10 μb/sr for the production of a pion in the $1s$ level. The experiment was able to place a limit of 350 μb/sr on the process.

In Sec. II we present the main ingredients of the distorted-wave formalism. A schematic plane-wave calculation is introduced in Sec. III as an aid to study the general dependencies. A more realistic distorted-wave calculation is outlined in Sec. IV, and results are presented in Sec. V. A discussion of experimental background processes is given in Sec. VI.

II. DETAILS OF THE MODEL

Our model calculations are based on the DWIA. The basic equation is [18]

$$\frac{d\sigma}{d\Omega} = KC^2S|T(\mathbf{k}',\mathbf{k})|^2 \tag{2}$$

where

$$T(\mathbf{k}',\mathbf{k}) = \int \psi_p^{(-)*}(\mathbf{k}',\mathbf{r})\,\phi_\pi^*(\mathbf{r})\,t(E_{\text{c.m.}};\mathbf{p}_\pi,\mathbf{k}_p;\mathbf{p}_p,\mathbf{k}_\pi) \times\phi_p(\mathbf{r})\,\psi_\pi^{(+)}(\mathbf{k},\mathbf{r})d^3r. \tag{3}$$

In these expressions $\psi_\pi^{(+)}(\mathbf{k},\mathbf{r})$ and $\psi_p^{(-)}(\mathbf{k}',\mathbf{r})$ are the initial pion and final nucleon scattering wave functions, and $\phi_\pi(\mathbf{r})$ and $\phi_p(\mathbf{r})$ are the pion atomic wave function and the initial proton bound-state wave function. $t(E_{\text{c.m.}};\mathbf{p}_\pi,\mathbf{k}_p;\mathbf{p}_p,\mathbf{k}_\pi)$ is the pion-nucleon transition operator, where $\mathbf{k}_\pi$ and $\mathbf{k}_p$ are the incident pion and outgoing proton momentum operators, $\mathbf{p}_p$ is the momentum operator of the struck proton, and $\mathbf{p}_\pi$ is the momentum operator of the bound pion in the final state. $\mathbf{k}$ and $\mathbf{k}'$ are the on-shell momenta of the incident pion and outgoing proton. C^2S is a spectroscopic factor, and the kinematic factor K is defined by [18]

$$K = \frac{\mu_\alpha\mu_\beta}{(2\pi)^2}\frac{k'}{k}, \tag{4}$$

where the reduced masses (energies) are given by

$$\mu_\alpha = \frac{m_\pi m_{\text{Nuc}}}{(m_\pi + m_{\text{Nuc}})}, \tag{5}$$

$$\mu_\beta = \frac{m_N m_{\mathrm{Nuc}'}}{(m_N + m_{\mathrm{Nuc}'})}. \tag{6}$$

m_{Nuc} and $m_{\mathrm{Nuc}'}$ refer to the initial and final nuclear masses. Because the pion and nucleon masses are small compared with the nuclear ones, we will approximate the reduced masses by m_π and m_N. For a relativistic correction, the masses are replaced by the corresponding energies in the projectile-nucleus center-of-mass frame.

The major ingredients will be discussed in turn.

A. The transition operator

The transition operator is the pion-nucleon elastic t matrix,

$$t(E_{\mathrm{c.m.}}; \mathbf{p}_\pi, \mathbf{k}_p; \mathbf{p}_p, \mathbf{k}_\pi) = -\frac{2\pi}{\mu}[a(E_{\mathrm{c.m.}}) + b(E_{\mathrm{em}})\boldsymbol{\kappa}\cdot\boldsymbol{\kappa}' + i\,c(E_{\mathrm{c.m.}})\,\boldsymbol{\sigma}\cdot\boldsymbol{\kappa}\times\boldsymbol{\kappa}'] \tag{7}$$

where $E_{\mathrm{c.m.}}$ is the pion-nucleon center-of-mass energy,

$$\boldsymbol{\kappa} = (m_p\mathbf{k}_\pi - m_\pi\mathbf{p}_p)/(m_p + m_\pi) \tag{8}$$

is the initial momentum, and

$$\boldsymbol{\kappa}' = (m_p\mathbf{p}_\pi - m_\pi\mathbf{k}_p)/(m_p + m_\pi) \tag{9}$$

is the final momentum in the center-of-mass system. The operators $\boldsymbol{\kappa}$ and $\boldsymbol{\kappa}'$ have been written in the Galilean invariant form, so that the momenta of the individual particles may be evaluated in the laboratory frame. μ is the reduced mass (energy) of the pion-nucleon system: $\mu = \frac{m_\pi m_N}{(m_\pi + m_N)}$. As before we normally replace the masses by energies in these expressions to partially account for relativistic kinematics. $E_{\mathrm{c.m.}}$ and the on-shell values of the momenta of the incident pion and outgoing proton are always calculated relativistically. The s and p wave contribution to t will be sufficient for the relatively low-energy pion beams we will consider. The coefficients a, b, and c are obtained directly from the pion-nucleon phase shifts:

$$a = \frac{1}{3}(2a^0_1 + a^0_3), \tag{10}$$

$$b = \frac{1}{3}(2a^1_{11} + 4a^1_{13} + a^1_{31} + 2a^1_{33}),$$

$$c = \frac{1}{3}(2a^1_{11} - 2a^1_{13} + a^1_{31} - a^1_{11}), \tag{11}$$

where $a^\ell_{2I\,2J} = (\eta^\ell_{IJ}\,e^{2i\delta^\ell_{IJ}} - 1)/2ik^{2\ell+1}_{\mathrm{c.m.}}$, and $k_{\mathrm{c.m.}}$ is the on-shell center-of-mass momentum of the pion-nucleon system. (Naturally, we have $2J = 1$ if $\ell = 0$.) The phase shifts, δ^ℓ_{IJ}, and inelasticity parameters, η^ℓ_{IJ}, are taken from the SAID compilation [19]. We have included the spin-flip amplitude in the plane-wave impulse calculation in order to verify that it is unimportant. It has been omitted from the distorted-wave calculation.

We have also omitted the Coulomb contribution to the transition operator, which is expected to be much smaller than that of the strong amplitude. The Coulomb potential is, of course, included in the computation of the distorted waves.

The entire calculation was performed in coordinate space, so that the momentum operators appearing in t become $(-i)$ times gradients on the appropriate wave functions. For example, $\mathbf{p}_\pi$ will act upon $\phi_\pi(\mathbf{r})$, and $\mathbf{k}_p$ will act upon $\psi^{(-)}_p(\mathbf{k}', \mathbf{r})$. The finite-range of the pion-nucleon transition operator is not included, although it is included in the pion distorted wave. See Sec. II C below.

B. The spectroscopic factor

After computing the cross section for the knockout of a proton from a particular shell, we must multiply it by the number of protons in the shell, the occupancy. For a ^{58}Ni target the $f_{7/2}$ shell is full, so we would expect to multiply the single-particle cross section by 8. When an $f_{7/2}$ proton is removed the final nuclear state may be any of a number of $7/2^+$ levels in the product nucleus ^{57}Co. If the experiment has sufficient resolution to pick out definite final states, say the ground state, then we must also multiply by the fraction of processes which leave the product nucleus in its ground state. The product of the occupancy and the fraction leading to a specific final state is the spectroscopic factor, C^2S, for the transition. This quantity has been determined by pickup reactions such as (t,α) or $(d,{}^3\mathrm{He})$. The spectroscopic factor for ^{58}Ni is 5.5 from the (t,α) experiment and 4.27 from the $(d,{}^3\mathrm{He})$ reaction leading to the ground state of ^{57}Co. The remaining strength 2.5 $(= 8 - 5.5)$ is spread among various other levels, the largest contribution being 1.37 for the $7/2^+$ level at excitation energy 1.89 MeV. The maximum strength for proton knockout from the $2s_{1/2}$ level is 2, with 1.31 concentrated in the $1/2^+$ level of ^{57}Co at 2.97 MeV. The rest of the strength lies somewhat higher in energy. The Nuclear Data Sheets are an excellent reference for spectroscopic factors for a variety of nuclei [20].

C. The initial pion scattering wave function

We have used a medium-corrected finite-range optical potential to compute the incident pion wave function [21]. The off-shell pion-nucleon range used was 300 MeV/c. The potential includes a phenomenological term to account for true absorption of the pion [22]. A run with off-shell range of 600 MeV/c was also made at 30 MeV

incident pion energy, and another with the absorption parameter doubled (at the upper end of what is consistent with the true absorption data). These calculations gave the same general angular behavior as the standard calculation, with the values differing of the order of 10%. Thus the predictions are rather resilient with respect to the choice of pion distorted wave.

D. The bound pion wave function

The bound pion wave function is a solution to the Klein-Gordon equation with the same optical potential as used in Sec. II C. The absorption parameter has been adjusted to give agreement with the observed widths of the higher levels. The Coulomb interaction is that of a uniform charged sphere of radius $1.2A^{1/3}$ fm. We have also used a second and simpler model: a pion in a real Woods-Saxon potential of radius $1.2A^{1/3}$ fm, diffusivity of 0.6 fm, and strength (replusive) +16 MeV [23]. The results of the atomic formation calculations are very close for the two different models (See Fig. 7). To get a feeling for the magnitudes, the binding energy of a $1s$ pion in ^{57}Co is approximately 1.58 MeV. If the strong interaction is turned off, this is increased to 2.24 MeV, (the s-wave interaction is repulsive). If the quadratic Coulomb term is also dropped in the Klein-Gordon equation, we get 2.32 MeV, so this correction is quite small. The Bohr result, good for a point nucleus, is 2.70 MeV.

E. The bound state nucleon wave function

The bound proton wave function satisfies a Schrödinger equation with a Woods-Saxon potential of radius $1.3A^{1/3}$ fm and diffusivity 0.5 fm. The Coulomb potential is taken to correspond to a uniformly charged sphere of the same radius. The depth of the potential well was chosen to give the last proton the experimental value of its separation energy. In the case of ^{58}Ni a potential depth of -53.4 MeV produces a proton separation energy of 8.16 MeV.

F. The final nucleon scattering wave function

The outgoing proton wave function was calculated with various different phenomenological proton-nucleus optical potentials [24]. We have omitted the small, real, spin-orbit portion of the potential.

III. THE PLANE-WAVE IMPULSE APPROXIMATION

Although the initial and final state interactions ("distortions") are very important for the (π^-,p) reaction, and we will include them shortly, insight into the dynamics can be obtained from a study of the plane-wave impulse approximation (PWIA), where the initial pion and final nucleon are described by plane waves. As mentioned in Sec. II A, the momentum operators appearing in $t(E_{\rm c.m.};\mathbf{p}_\pi,\mathbf{k}_p;\mathbf{p}_p,\mathbf{k}_\pi)$ are -i times a gradient operator acting on the wave function associated with the momentum. For example, the gradient associated with $\mathbf{k}_\pi$ acts on the incident pion's wave function. For a plane wave the result of the operation is simply $\mathbf{k}$, the on-shell momentum of the incident pion. Similarly, $\mathbf{k}_p$ becomes $\mathbf{k}'$, the on-shell value of the outgoing proton. The momentum operators associated with the bound particles, $\mathbf{p}_\pi$ and $\mathbf{p}_p$, are gradients of the pionic atom wave function and of the inital shell-model proton wave function. The terms in t involving these momenta turn out to be rather small and we will drop them here. They will be included in the full DWIA calculation outlined in the next section. The plane-wave amplitude is

$$T(\mathbf{k}',\mathbf{k}) = t(\mathbf{k},\mathbf{k}')\int e^{-i\mathbf{k}'\cdot\mathbf{r}}\phi_\pi^*(\mathbf{r})\phi_p(\mathbf{r})e^{i\mathbf{k}\cdot\mathbf{r}}d^3r \tag{12}$$

where $\phi_p(\mathbf{r}) = \phi_{n_p\ell_p}(r)Y_{\ell_p m_p}(\hat{\mathbf{r}})$ is the initial bound proton wave function and $\phi_\pi(\mathbf{r})$ is the final bound pion wave function. Performing the integrals, squaring, averaging over m_p, and summing over m_π, we find

$$\frac{d\sigma}{d\Omega} = K\,C^2\,S\left|t(\mathbf{k}',\mathbf{k})\sum_L F_L(\mathbf{q}^2)\begin{pmatrix} L & \ell_\pi & \ell_p \\ 0 & 0 & 0\end{pmatrix}\sqrt{2L+1}\right|^2 (2\ell_\pi+1) \tag{13}$$

where

$$F_L(q^2) = \int_0^\infty j_L(qr)\phi_{n_\pi\ell_\pi}(r)\phi_{n_p\ell_p}(r)r^2dr \tag{14}$$

is the transition multipole form factor. The kinematic factor K was defined in the preceding section. If either ℓ_π or ℓ_p is zero then only one L survives. For example, for $\ell_\pi = 0$ we have

$$\frac{d\sigma}{d\Omega} = K\,C^2\,S\,\left|t(\mathbf{k}',\mathbf{k})\,F_{\ell_p}(\mathbf{q}^2)\right|^2. \tag{15}$$

The momentum transfer is defined by $q^2 = (\mathbf{k}-\mathbf{k}')^2 = k^2 + k'^2 - 2kk'cos\theta$, where θ is the angle between the outgoing proton and the incoming pion. The physical values of q are confined between $k_{\rm min} = |k-k'|$ and $k_{\rm max} = |k+k'|$. If the nucleon is coupled to a definite (n,ℓ,j) the expression is unchanged provided that the spin-flip contribution to the transition operator is negligible.

Figure 2 shows $F_{\ell_p}(q^2)$ for various shells (using nuclear notation): $1s$, $1p$, $1d$, and $1f$. If the incident pion energy is 10, 20, 30, or 40 MeV, the kinematic limits on q are (0.33,0.93), (0.46,1.32), (0.53,1.63), or (0.61,1.88) fm^{-1}, respectively, assuming that the Q value of the reaction is zero (i.e., the original binding energy of the proton is the same at the atomic binding energy of the pion). The

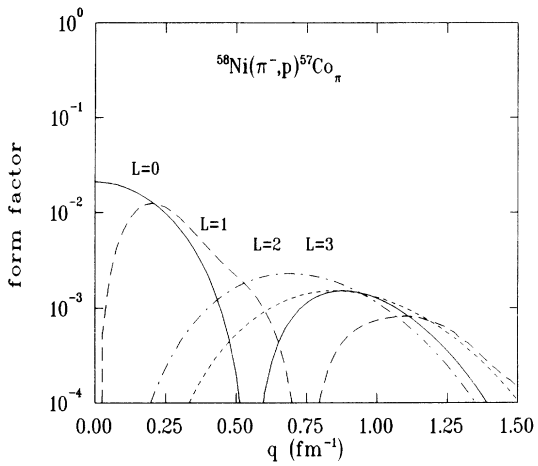

FIG. 2. Plane-wave form factors, $F_\ell(q^2)$. The range of physical values of q as a function of incident pion energy is given in the text. Because of the unequal-mass kinematics and the nonzero Q values the forward form factor does not correspond to q=0. Because these are transition form factors, the value of the monopole form factor at q=0 is less than one.

band of allowed momentum transfer expands and moves upward as the energy of the incident beam increases. Consequently, as the incident energy rises, the process selects successive shells. Even at rather low energies an angular momentum mismatch is often an advantage if the transition involves a difference in nucleon and pion bound-state angular momenta. This explains how in the case of ^{58}Ni, for which the proton $f_{7/2}$ shell is full, the cross section peaks at back angles for low incident pion energies and at forward angles for high incident energies. There is an optimum value of the energy, somewhere near 30 MeV for which the form factor peaks well within the physical region. Because the different multipoles peak at different energies, a single multipole tends to dominate for any particular energy and angle. The pion-nucleon t matrix $t(\mathbf{k}',\mathbf{k})$ modulates the form factor. At 30 MeV the $\pi^- p$ elastic cross section peaks with the pion in the forward direction; this corresponds to backward knock-out of the proton. It is therefore an advantage that the form factor peaks at larger angles where the elementary cross section is greater.

IV. THE DISTORTED WAVE IMPULSE APPROXIMATION

In reality both the pion and proton waves are strongly affected by the nuclear medium. This interaction will be taken into account through the DWIA. The DWIA integral is most conveniently calculated in terms of partial waves. The bound-state wave functions already have definite angular momenta. The incident pion and outgoing proton wave functions are

$$\psi^{(+)}(\mathbf{k},\mathbf{r}) = 4\pi \sum_{\ell m} i^\ell \psi_\ell^{(+)}(k,r)\, Y_{\ell m}(\hat{\mathbf{r}}) Y_{\ell m}(\hat{\mathbf{k}})^*, \tag{16}$$

$$\psi^{(-)}(\mathbf{k}',\mathbf{r}) = 4\pi \sum_{\ell' m'} (-i)^{\ell'} \psi_{\ell'}^{(-)}(k',r) \times Y_{\ell' m'}(-\hat{\mathbf{r}}) Y_{\ell' m'}(\hat{\mathbf{k}'})^*. \tag{17}$$

The radial wave functions, $\psi^{(+)}(k,r)$ and $\psi^{(-)}(k',r)$ are determined by the solution of the Schrödinger equation for the proton and by the solution of the radial Klein-Gordon equation for the pion as is outlined in Sec. II. In the following we will assume that the pion is in the $1s$ state. The contribution coming from the s-wave portion of the transition operator is proportional to

$$(-i)^{\ell-\ell'}\ (2\ell+1)(2\ell'+1)\sqrt{2\ell_p+1} \begin{pmatrix} \ell_p & \ell & \ell' \\ 0 & 0 & 0 \end{pmatrix} \begin{pmatrix} \ell_p & \ell & \ell' \\ m_p & 0 & -m_p \end{pmatrix} F_{\ell\ell'}(k,k') Y_{\ell' m_p}(\theta,0). \tag{18}$$

The distorted-wave form factors are

$$F_{\ell\ell'}(k,k') = \int_0^\infty \psi_{\ell'}^{(-)}(k',r)^*\ \phi_{n_\pi \ell_\pi}(r) \phi_{n_p \ell_p}(r)\ \psi_\ell^{(+)}(k,r)\ r^2 d\mathbf{r}, \tag{19}$$

z is chosen along the beam axis. x is chosen so $\mathbf{k}'$ lies in the x-z plane. The 3-j symbols result from the integral over three spherical harmonics. The sum of this term and its p-wave counterpart is summed over ℓ and ℓ', squared, and averaged over m_p.

The p-wave contribution, although more complicated, can be reduced to nearly the same form. The momentum operators appearing in t cannot be replaced by their on-shell values now, and the gradients must be calculated. From Sec. II A the contribution consists of four terms:

$$b(E_{\text{c.m.}})\, \lambda^2 (\mathbf{k}_\pi \cdot \mathbf{p}_\pi - \rho \mathbf{p}_p \cdot \mathbf{p}_\pi - \rho \mathbf{k}_\pi \cdot \mathbf{k}_p + \rho^2 \mathbf{p}_p \cdot \mathbf{k}_p) \tag{20}$$

where $\lambda = m_p/(m_p+m_\pi)$ and $\rho = m_\pi/m_p$. When this expression is substituted into the distorted-wave integral the terms in Eq. (20) become

$$\int \nabla \phi_\pi^*(\mathbf{r}) \cdot \nabla \psi_\pi^{(+)}(\mathbf{k},\mathbf{r})\, \psi_p^{(-)*}(\mathbf{k}',\mathbf{r})\, \phi_p(\mathbf{r})\, d^3\mathbf{r}, \tag{21}$$

$$-\rho\int \nabla\phi_\pi^*(\mathbf{r})\cdot\nabla\phi_p(\mathbf{r})\,\psi_p^{(-)*}(\mathbf{k}',\mathbf{r})\,\psi_\pi^{(+)}(\mathbf{k},\mathbf{r})d^3\mathbf{r}, \tag{22}$$

$$-\rho\int \nabla\psi_p^{(-)*}(\mathbf{k}',\mathbf{r})\cdot\nabla\psi_\pi^{(+)}(\mathbf{k},\mathbf{r})\,\phi_\pi^*(\mathbf{r})\,\phi_p(\mathbf{r})\,d^3\mathbf{r}, \tag{23}$$

$$+\rho^2\int \nabla\psi_p^{(-)*}(\mathbf{k}',\mathbf{r})\cdot\nabla\phi_p(\mathbf{r})\,\psi_\pi^{(+)}(\mathbf{k},\mathbf{r})\phi_\pi^*(\mathbf{r})\,d^3\mathbf{r}. \tag{24}$$

Rather than use the gradient formula [25] to evaluate these expressions, we proceed as follows. The dot product of two gradients multiplied by a function and integrated over all space can be rewritten using the following vector identity:

$$\int cd\,\nabla a\cdot\nabla b\,d^3r$$

$$=\frac{1}{2}\int[cd\,\nabla^2(ab)-acd\,\nabla^2 b-bcd\,\nabla^2 a]\,d^3\mathbf{r}, \tag{25}$$

where a, b, c, and d are arbitrary functions of $\mathbf{r}$. There are now twelve ($=3\times4$) terms in the sum rather than four, but the advantage is that the gradient operators now appear only as Laplacians. Consequently, the angular-momentum algebra is the same as that encountered for the s-wave amplitude. The only difference between individual p-wave and s-wave terms is that the distorted-wave form factors for the p-wave case involve derivatives of the radial wave functions.

V. RESULTS

Because the atomic wave function is so extended, low Z nuclei such as carbon have small cross sections for the pion capture reaction. Fortunately, the $1s$ and $2p$ levels of such light nuclei can already be seen through the x-ray cascade. Plane-wave calculations of very high Z nuclei give large cross sections, but these nuclei also create large distortions in both pion and proton waves, so that the cross sections which seemed promising in the PWIA are severely diminished. A reasonable strategy for an exploratory experiment would be to avoid the extremes of large distortions (large Z) and small atomic-nuclear overlap (small Z). The ideal would be a medium mass which has a large spectroscopic factor concentrated in a single or a few levels.

Without any systematic optimization we have chosen as a target ^{58}Ni. The product nuclear-atomic system, after proton knockout will be $(^{57}\mathrm{Co})_\pi$, where the pion is in the $1s$ state. Figures 3, 4, and 5 give the cross sections for the process at 20 MeV, 30 MeV, and 50 MeV. At 30 MeV the cross section is peaked at about 40–50 degrees from the beam direction. At higher incident pion energies the peak moves more forward as was already seen in the plane-wave model, and above 50 MeV the cross section drops rapidly. At these lower energies the cross sections are small, but not prohibitively so, of the order of a microbarn per steradian. The integrated cross section is of the order of 10–20 μb.

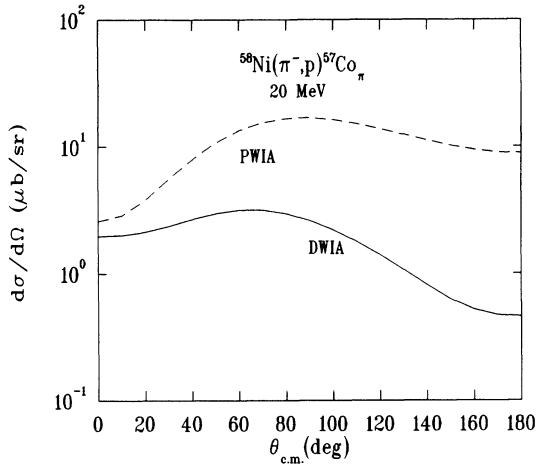

FIG. 3. Pion-capture to the $1s$ atomic level. $T_{\pi^-}=20$ MeV. The effect of distortions is to greatly lower the cross section.

At 160 MeV the cross section is very strongly forward peaked, and of the order of 1 μb/sr in the forward direction. The higher-energy process has the advantage that the background is probably smaller; see the comments at the end of Sec. VI.

The distortions of the pion and proton waves together lower the cross section by approximately an order of magnitude. The model dependence due to the choice of proton-nucleus optical potentials is illustrated in Fig. 4.

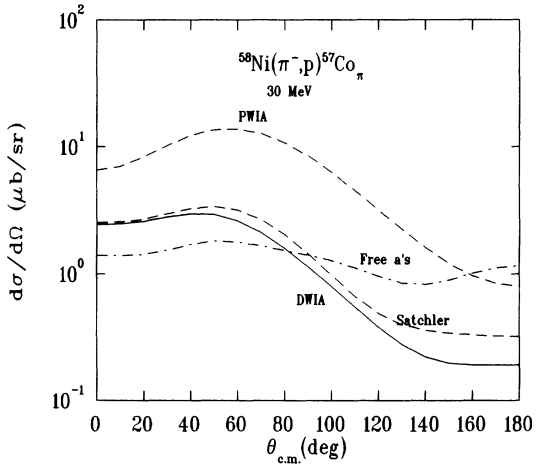

FIG. 4. Pion-capture to the $1s$ atomic level. $T_{\pi^-}=30$ MeV. The solid line uses modern parameters for the distorted waves. The curve marked "Satchler" uses the proton distorted wave calculated from the first item in Ref. [22]. The dependence is seen to be rather minor. The curve marked "Free a's" completely ignores medium corrections in the pion distorted wave. The medium corrections at low pion energies increase the transparency of the nucleus to pions and enhance the forward cross section.

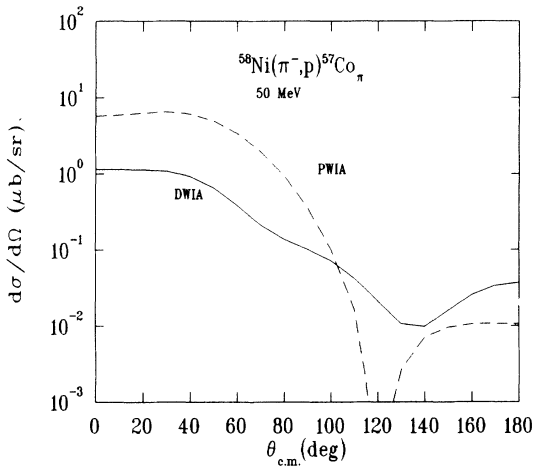

FIG. 5. Pion-capture to the $1s$ atomic level. T_{π^-}=50 MeV.

Substantial quantitative differences are evident, but the results are in general qualitative agreement. The curve labeled "free strengths" results from a pion optical potential for the incident π^- whose parameters are determined directly from the pion-nucleon amplitudes without any medium corrections, which make the pion-nucleus optical potential somewhat less absorptive in this energy regime. The medium corrections thus produce a modest increase in the predicted cross sections.

The curves in Fig. 6 represent calculations in which (1) both pion and nucleon waves are distorted, (2) only the pion wave is distorted, (3) only the nucleon wave function is distorted, or (4) neither wave is distorted. The majority of the degradation of the cross section is seen to come from the distortions of the nucleon. It is curious that in the backward direction the cross section is greater with both waves distorted than with either one independently distorted.

Figure 7 indicates the model dependence on the atomic wave function. All calculations were done with fully distorted pion and proton scattering wave functions. The effect of the finite size of the nuclear charge distribution is to lower the cross section substantially. This dependence is probably due to the greater overlap of the proton and pion wave functions when a point-Coulomb wave function is used. Since the repulsive s-wave strong interaction makes the pion atomic wave function more extended, the cross section becomes even smaller when it is included. If the expected repulsion is not present, the cross sections would be greater than 10 μb/sr in the forward direction. The cross sections calculated using the full pion-nucleus nonlocal optical potential and that calculated using the simple Woods-Saxon models give rather similar results.

As mentioned in the introduction, the cobalt nucleus could also be produced in an excited state. The cross sections for the ground state and the two most strongly excited states are shown in Fig. 8. The cross sections to the lowest lying $3/2^+$ is quite small; at least in the forward direction the cross section to the lowest $\frac{1}{2}^+$ state is comparable to the ground state production. Because of the different Q values, the curves correspond to different final state proton energies, and so the cases can be separated experimentally.

We have also calculated the cross section for the case where the pion knocks out a neutron rather than a proton, the product nucleus being ^{57}Ni. The neutron optical potential yielding the neutron distorted wave was taken from the compilation of Perey [24]. The angular distributions for an incident energy of 30 MeV are shown in Fig. 9. The cross section to the ground state is forward

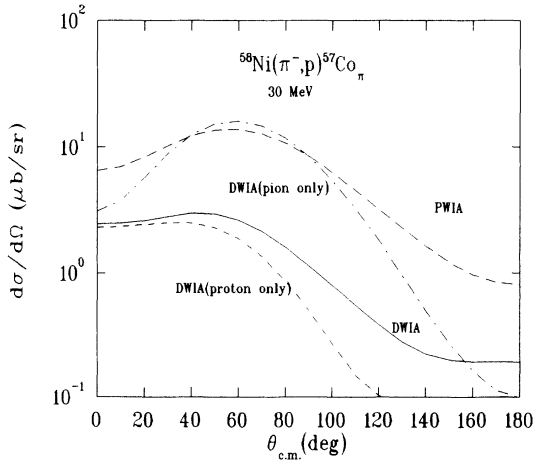

FIG. 6. The effect of pion and proton distorted waves. The four curves correspond to distortions on both pion and proton wave functions: pion only, proton only, or neither. Both distortions are seen to be rather important, but the nucleon distortions are the most significant.

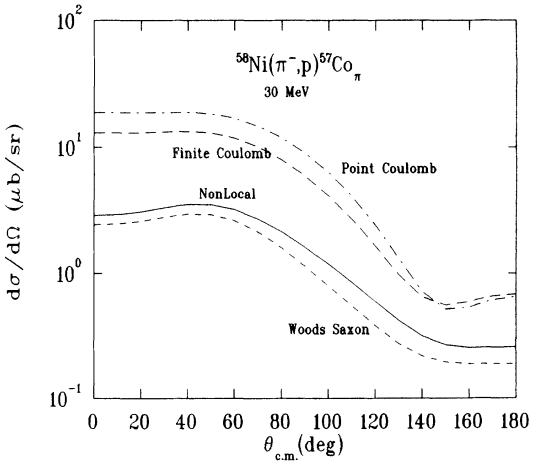

FIG. 7. Dependence on the pion atomic wave function. The upper two curves include only Coulomb interaction in the pion atomic wave function, while the lower pair also include the strong interaction. The distorted waves and bound proton wave function are the same as in Figs. 3–5. Cf. Fig. 1 where it is clear that the rms radii of the "Coulomb only" atomic wave functions are smaller than those which also include the strong interactions.

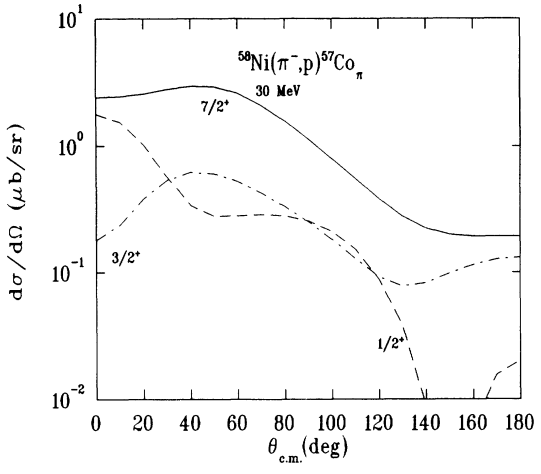

FIG. 8. Pion-capture to the $1s$ atomic level with the nucleus left in an excited state. The solid line corresponds to the nucleus left in the $7/2^+$ ground state. The cross sections corresponding to the final-state nucleus ^{57}Co left in the $J = 3/2^+$ and $J = 1/2^+$ states, denoted by dot-dashed and dashed lines respectively, are seen to be somewhat smaller.

peaked and is nearly an order of magnitude larger than the case in which the proton is ejected. That the neutron knockout cross section is larger than the proton can be attributed to the larger elementary $\pi^- n$ amplitude, which is pure $T = \frac{3}{2}$. Furthermore, at 30 MeV the elastic $\pi^- n$ cross section is peaked for the pion in the backward direction, and hence the forward direction is favored for the knockout neutron. Figure 8 also shows the calculated cross section for the process in which ^{57}Ni is left in the $7/2^+$ excited state. It is also large and dominates at larger angles. Even if there were insufficient energy resolution to separate the ground state from the $7/2^+$, an experiment which could measure this angular distribution could make a meaningful statement about the pion

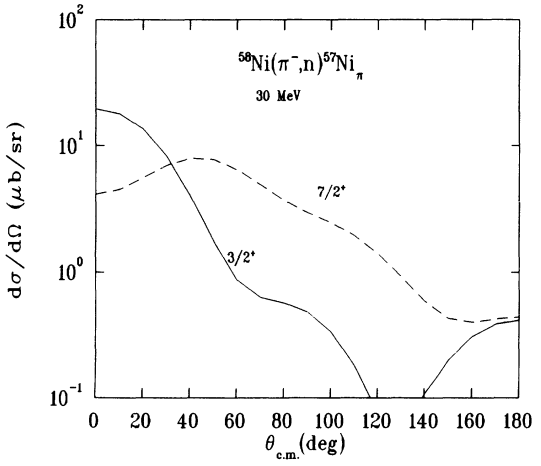

FIG. 9. Pion-capture to the $1s$ atomic level via neutron knockout. The cross sections are seen to be somewhat larger than in the case of proton knockout. Unfortunately, experimental problems are greater in this case.

optical potential for an excited nucleus. Unfortunately, a neutron is much harder to observe than a proton, so the proton knockout reaction may be experimentally preferable.

VI. CONSIDERATIONS OF EXPERIMENTAL BACKGROUND

The cross sections calculated here for the production of pionic atoms are not large but neither are they small by modern standards, being of the same order as pion double charge exchange. The principal difficulty would seem to be that of the proton background. Protons coming from direct knockout do not present a significant problem since their energies must lie below the energy of the final-state proton following pionic-atom formation, but protons produced in the absorption process can have energies in this region. Pionic absorption will produce a continuous spectrum of neutrons and protons. While the primary mechanism will tend strongly to produce two neutrons, secondary knockout reactions and charge exchange will produce protons from the initial neutrons giving two sources of background protons, those coming from the direct absorption on a proton-proton pair and those produced in secondary reactions (within the same nucleus). The second component is more difficult to estimate, even given the basic absorption cross section.

For low energies of the incident π^- beam (around 30 MeV) the Coulomb potential of the nucleus causes the interaction cross section to become large and hence enhances the absorption cross section. The only measurement on heavy nuclei at low energy is the indirect one by Nakai *et al.* [26]. These authors extracted pionic absorption cross sections from the measurement of gamma rays from nuclei far removed (in A) from the target. In this region of pion energies, processes exist that are not classical absorptions. For example a pion can undergo a quasi-free scattering in which it loses a significant amount of energy and is trapped in the atomic potential (in some very high level) and then, once again, passes by the nucleus and is absorbed. This mechanism is not included in the usual optical-model theories but does represent a "true" absorption in the sense that it takes place on a single nucleus (and atom). A process that creates an uncertainty in the estimation of background is that of an absorption in a second atomic system after a large energy loss in a first quasifree interaction. Such a process depends on target thickness and since the measurements of Nakai *et al.* were made with thick targets there may be a significant component of this mechanism in the data (if it is important). From this discussion we may draw two conclusions. First, the background is best determined by measurements designed for this purpose, and, second, the background may be smaller at higher energies (in the delta resonance region) contrary to naive expectations.

VII. CONCLUSIONS

Do the deeply bound pionic states such as the 1s state in medium to heavy mass nuclei actually exist? Current optical-potential calculations suggest that they do. In

this view, the states are not observed simply because the pions are annihilated too early in the normal atomic x-ray cascade process. Over more than 20 years many production mechanisms have been suggested for producing these states, but none have yet succeeded experimentially. The payoff will be a unique window on the low-energy pion-nucleus interaction.

In this article we have investigated the direct-pion-capture reaction $\pi^- + (N, Z+1) \rightarrow p + (N, Z)_{\pi^-}$ suggested by Birbriar *et al.* [14]. It appears to be a promising candidate to populate these deep pionic levels. The mechanism is also capable of producing pionic atoms in which the nucleus is excited. We have focused on a medium mass nucleus, Ni, for this study. For pions in the energy range 20–50 MeV the cross section for a Ni target is of the order of a few microbarns per steradian at forward angles, well within the capabilites of modern meson factories. The most significant experimental challenge is to distinguish the knockout proton from those ejected following pion annihilation.

ACKNOWLEDGMENTS

We thank M. W. Rawool-Sullivan for many conversations about the experimental aspects of this reaction. This work was supported in part by the United States Department of Energy.

[1] The x-ray spectra from the formation of pionic atoms were first observed by M. Camac, A. D. McGuire, J. B. Platt, and J. H. Schulte, Phys. Rev. **88**, 897 (1952). There were also earlier indications of the existence of pionic atoms. See the old, excellent review of pionic atoms by G. Backenstoss, Annu. Rev. Nucl. Sci. **20**, 467 (1970).

[2] We use the atomic convention, where $2p$ is the lowest p state.

[3] See, for example, the review, *Pionic Atoms* by J. Konijn, presented at the Fourth International Oberjoch Meeting on Pion-Nuclear Physics, Oberjoch, Germany, 1991 (unpublished).

[4] H. Toki and T. Yamazaki, Phys. Lett. B **213**, 129 (1988).

[5] H. Toki, S. Hirenzaki, T. Yamazaki, and R. S. Hayano, Nucl. Phys. **A501**, 653 (1989).

[6] H. Toki, S. Hirenzaki, T. Yamazaki, and R. S. Hayano, Nucl. Phys. **A527**, 455c (1991).

[7] C. Tzara, Nucl. Phys. **B18**, 246 (1970).

[8] G. T. Emery, Phys. Lett. **60B**, 351 (1976).

[9] T. Yamazaki, Nucl. Phys. **A518**, 213 (1990). The article contains a summary of much of the lore of deeply bound pionic atoms. It also has an extensive set of references.

[10] J. Nieves, E. Oset, and R. C. Carrasco, in *International Workshop on Pions in Nuclei*, Peñiscola, Spain, 1991, edited by E. Oset, M. J. Vincente Vacas, and C. García Recio (World Scientific, Singapore, 1992).

[11] M. V. Kazarnovskii, B. V. Krippa, and Yu. M. Nikolaev, in *International Workshop on Pions in Nuclei* [10].

[12] T. Yamazaki, R. S. Hayano, and H. Toki, Nucl. Instrum. Methods **A305**, 406 (1991).

[13] W. B. Amian *et al.*, in *Experimental Investigation of Low-Lying States of Pionic Atoms*, Particle Production Near Threshold, AIP Conf. Proc. No. 221, edited by H. Nann and E. Stephenson (AIP, New York, 1991). See also the article by J. Nieves and E. Oset in the same volume.

[14] A. B. Gridnev, private communication to T. Yamazaki, quoted in T. Yamazaki, Nucl. Phys. **A518**, 213 (1990). The latter article contains many references to earlier work. See also B. L. Birbriar, A. B. Gridnev, and Yu. A. Kalashnikov, ETHZ-IMP Internal Report 91-2, April 1991.

[15] M. W. Rawool-Sullivan and C. M. Morris, private communication.

[16] W. R. Gibbs and W. B. Kaufmann, Phys. Lett. **145B**, 1 (1984).

[17] M. Iwasaki *et al.*, Phys. Rev. C **43**, 1099 (1991).

[18] N. Austern, *The Direct Theory of Nuclear Reactions* (Wiley-Interscience, New York, 1970), Eqs. 1.31 and 1.32. See also J. M. Eisenberg and D. S. Koltun, *Theory of Meson Interactions with Nuclei* (Wiley, New York, 1980).

[19] SAID computer program, R. Arndt *et al.*, Virginia Polytechnic Institute and State University, Blacksburg, VA 24061.

[20] For ^{58}Co see T. W. Burrows and M. R. Bhat, Nucl. Data Sheets **47**, 101 (1986).

[21] W. B. Kaufmann and W. R. Gibbs, Phys. Rev. C **28**, 1286 (1983).

[22] M. Leitch *et al.*, Phys. Rev. C **39**, 2356 (1989).

[23] Frank Valdovinos, private communication.

[24] G. R. Satchler, Nucl. Phys. **A92**, 273 (1967), R. C. Barrett, A. D. Hill, and P. E. Hodgson, Nucl. Phys. **62**, 133 (1965); C. M. Perey and F. G. Perey, At. Data Nucl. Data Tables **13**, 293 (1974). In the latter, we have used the generic parameters of J. J. H. Menet, E. E. Gross, J. J. Malanify, and A. Zucker, Phys. Rev. C **4**, 1114 (1971). For the 160 MeV proton wave function we have used the optical potential of P. Schwandt *et al.*, *ibid.* **26**, 55 (1982).

[25] M. Rotenberg, *3-j and 6-j Symbols* (Cambridge University Press, MIT, 1959).

[26] K. Nakai *et al.*, Phys. Rev. Lett. **44**, 1446 (1980).